

Article

Adaptation of a High-Pressure Liquid Chromatography System for the Measurement of Viscosity

Sonia Gregory and Henryk Mach *

Merck Research Laboratories, Merck & Co., Inc., West Point, PA 19486, USA;

E-Mail: henryk.mach@merck.com

* Author to whom correspondence should be addressed; E-Mail: henryk.mach@merck.com;
Tel.: +1-215-652-4689; Fax: +1-215-993-1750.

Received: 27 January 2014; in revised form: 10 March 2014 / Accepted: 17 March 2014 /

Published: 26 March 2014

Abstract: The state-of-the-art instruments for the determination of viscosity of liquids typically require a significant amount of sample, and have relatively low throughput due to manual and sequential measurements. In this study, it was demonstrated that the pressure generated by the flow of viscous fluids through a capillary could be precisely measured employing high-pressure liquid chromatography systems (HPLC) using glycerol solutions of moderate viscosity as a mobile phase, and correlated to the dynamic (absolute) viscosity. The parameters allowing calculation of the viscosity of glycerol calibration standards as a function of temperature were established. The measurements were made with volumes as small as 10 μ L, and the use of an autosampler permitted unattended analysis of a large number samples. The method appears to be particularly well suited for the development of viscous formulations of therapeutic, protein-based macromolecules, where the amount sample is typically limited and relatively wide ranges of conditions are considered in the optimization process. The utility of the methods was illustrated by application to the development of concentrated inactivated virus vaccines.

Keywords: viscosity; high-pressure liquid chromatography; protein formulation

1. Introduction

Viscosity is an important practical parameter that often determines limits of processing and delivery, and yields useful information about the state and interactions of macromolecules [1–9].

In the realm of therapeutic protein and vaccine development, the relatively scarce amounts of sample available at the early research stages often hinder meaningful bioprocess design and formulation screening [7]. Originally viscosity measurements were based on the time that takes for a solution to flow through a glass capillary tube [10]. Nowadays, they are seldom used due to the time and effort required to make the measurements. More often, rheometers that measure not only the dynamic viscosity, but also shear forces are applied [11]. Falling ball viscometers capable of measuring a wide range of viscosity are also used [12]. A dynamic light scattering plate reader has also been used successfully to measure viscosity of concentrated protein solutions by utilizing the dependence of the diffusion coefficients of added sizing standards on solution viscosity [13]. More recently, a small volume viscometer based on a pressure measurement was developed [14], but still it is a manually operated instrument. In this report, we describe the use of commonly accessible HPLC systems, combined with low diameter tubing and a glycerol solution as a mobile phase for the determination of the viscosity of concentrated inactivated virus vaccine solutions. This development is likely to be applicable to both aqueous and organic solvent systems where sample preservation and throughput are important considerations.

2. Materials and Methods

2.1. High Pressure Liquid Chromatography (HPLC)

The Waters Alliance 2690 HPLC system (Millford, MA, USA) was equilibrated with ~70% glycerol in water as a mobile phase and the temperature was set to 25.0 °C. The outlet flow from the HPLC pump was connected using standard finger-tight HPLC connectors and a 50 cm section of PEEK tubing (0.005 inches inner diameter, 1/16 inches outer diameter, red-striped, Alltech, Deerfield, IL, USA). It is critical to minimize the dead volume between the injector and low diameter tubing. Preferably, the low diameter tubing should be connected directly to the injector. The tubing was held in a column heater at 25 °C. The outlet of the tubing was connected to a photo-diode-array (PDA) detector for collection of UV signals to potentially estimate the concentration as well as turbidity measurements indicative of the aggregation state of tested samples. In most cases, however, refractive index differences between the mobile phase and the samples precluded collection of valid UV signals. Empower[®] 2 software (Waters Corporation, Millford, MA, USA) was used to run the instruments and collect the data. The stroke volume was set 130 µL, syringe rate to “slow”, depth of needle to 0, pre-column volume to 0, and needle wash time to “extended”. Bubble detect and degas options were selected. High and low pressure limits were set to 4,000 psi and 0 psi, respectively. The isocratic flow was at 50 µL/mL, with acceleration rate setting at 10 mL/min in 2 min. 10 µL injections were used throughout. The raw chromatograms were exported to a Microsoft Excel[™] workbook for further processing. It should be noted that the time boundaries for peak integration depended on the particular tubing configuration. For example, replacing the tubing often required an adjustment of data processing parameters, followed by generation of a new calibration curve.

2.2. Materials

Glycerol (EM Science, Gibbstown, NJ, USA) dilutions in USP water were used as standards to set parameters and to create a calibration curve. A calibrated scale was used to measure the amounts of glycerol and water that were mixed to form the calibration solutions. Lyophilized bovine serum albumin (BSA) was purchased from Sigma-Aldrich (St. Louis, MO, USA). Inactivated and lyophilized Varicella vaccine samples were produced within Merck & Co. (Whitehouse Station, NJ, USA) and provided in 3 mL glass vials.

3. Results and Discussion

3.1. Optimization of Mobile Phase

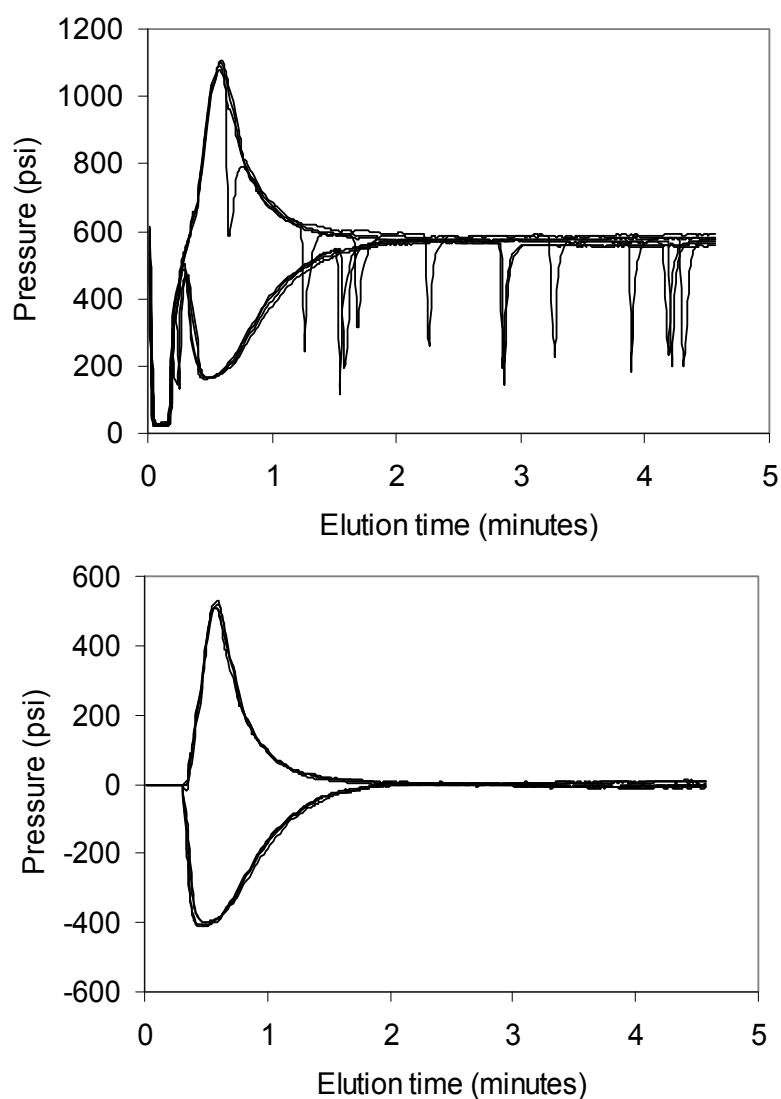
USP water was initially used as the mobile phase. However, the resulting pressure vs. log viscosity plots were linear only up to approximately 10 cP, and the noise became excessive at higher values (data not shown). Additionally, the minimal length of tubing required to generate sufficient pressure signal was approximately 3 m, thus requiring relatively large injection volumes (approximately 40 μ L) to fill that length of tube for precise backpressure measurements. The use of capillary tubing in combination with ultra high-pressure chromatography (UPLC) system was attempted, but the capillaries were prone to blocking due to the presence of sub-visible particles in highly concentrated protein formulations [15]. The problem of excessive noise for relatively viscous samples observed for the aqueous mobile phase buffer was solved by the use of 70% glycerol. With a flow rate of 0.05 mL/min, 0.005 inch internal diameter tubing at a length of 50 cm generated about 600 psi pressure when only mobile phase was run (shown in the later sections). Injection of liquids of lower viscosity such as water resulted in lower signal and injections of more viscous glycerol solutions generated signal approaching 2,000 psi. However, when highly concentrated protein solutions were injected, the signal decreased at the beginning and the end of the otherwise positive peaks, indicating that the water present in the injector tubing partially diffused into the sample during the injection (data not shown). Therefore, the injector system was re-equilibrated with the mobile phase (70% glycerol, ~20 cP), assuring efficient rinsing of the injector and at the same time precluding temporary changes of the pressure due to the introduction of small amounts of less viscous liquids during the injection.

3.2. Digital Removal of Pump Pulse Spikes

In typical HPLC pumps there are two pistons present, one that is pumping the mobile phase out of its chamber and into the system, and the other one moving in reverse direction while drawing the mobile phase into its chamber. When the pistons exchange their roles, a brief drop of the pressure occurs that is recorded by the transducer. The resulting spikes are seen in Figure 1. A trivial Microsoft Excel™ macro program was written using embedded Visual Basic that “zapped” the negative spike peaks. The program scanned each profile point by point, and when a sudden drop (>25% of signal magnitude) was encountered, backed up two points to establish starting point for the linear interpolation. The 14th consecutive data point was used as an ending point; thus, the “zapped” region spanned 14 s (one data point was acquired every second). The data shown in Figure 1 illustrates

the effectiveness of the zapping procedure as well as an excellent reproducibility of the method (four, essentially overlapping, runs are shown for each of the two samples). The effect of diffusion is also apparent, as the more viscous samples produced a narrower peak in comparison to less viscous ones. It should be noted that the exact concentration of glycerol in the running phase can vary over the long term due to water evaporation effects. The resulting back-pressure will also depend on the ambient temperature and the temperature in the thermostat, if used. For example, the calibration curves in the following figures intersect the zero line (where peak area is zero) at an apparent glycerol concentration of approximately 75%. Thus, injections of glycerol standards of well-controlled concentrations should be performed during the experiment to assure that the most recent calibration curve is valid.

Figure 1. Representative profiles of *water (lower curves)* and *90% glycerol (upper curves)*. The raw data is shown in upper panel, while the profiles after digital removal of pump pulse spikes are shown in lower panel. Average pressure values between 2 min and 3 min were subtracted from the raw data in upper panel to account for background back pressure in the system. See Materials and Methods section for experimental details.

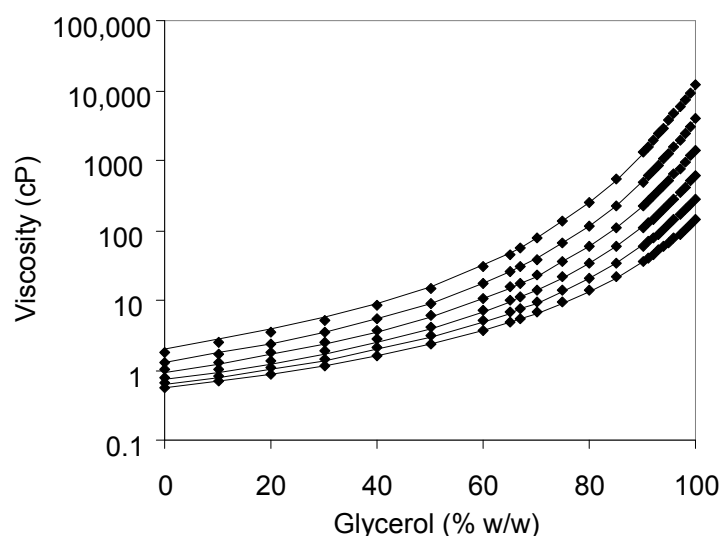


Generation of a standard curve for the measurement of viscosity using this method was performed using a series of glycerol aqueous solutions of various concentrations. The theoretical viscosity values were first calculated using the approach of Chang [16], and compared to experimental values published by Dow Chemical Company [17], and those given in the Handbook of Chemistry and Physics [18]. However, significant discrepancies were found between the calculated and listed values, e.g., the values for 80% glycerol at 25 °C were 45.9 cP and 47.0 cP at CRC and Dow Chemical tables, respectively, while the calculation method [16] yielded a value of 80.7 cP. Therefore, the Dow Chemical Company table was employed for the creation of the calibration curve. The values at 25 °C and at glycerol concentrations not listed at the original table were obtained by least-squares fitting to the relation [19]:

$$\eta = \exp(-B + DT + E_s/RT) \quad (1)$$

where η is dynamic viscosity, B and D are parameters, E_s is the activation energy of viscous flow of solution, R is the gas constant and T is absolute temperature. The data points used for fitting are shown in Figure 2.

Figure 2. The viscosities of glycerol solutions at various concentrations listed on the DOW Chemical Company web page at temperatures from 0 °C (top line) to 50 °C (bottom line). The solid lines represent best least-squares fits to Equation (1), using a value of 90 kJ/mol for the energy of activation of viscous flow (E_s).



The temperatures from 0 °C (top curve) to 50 °C (bottom curve) at 10 °C intervals were used. A constant value of 90 kJ/mol the activation energy of viscous flow was found to produce adequate fits, while the values of parameters B and D differed between the concentrations. The values of these parameters at different temperatures, as well as resulting values of dynamic viscosity at 25 °C calculated from Equation (1) are listed in Table 1.

Table 1. Parameters for the calculation of viscosity values of glycerol between 0 °C and 50 °C using Equation (1). The value for E_c (activation energy of viscous flow) was 90 kJ/mol. Viscosity values at 25 °C as calculated using Equation (1) are listed for convenience.

% (w/w)	B	D	$\eta_{25\text{ }^\circ\text{C}}$ (cP)
0	64.526	0.096595	0.89 *
10	64.526	0.094838	1.06
20	63.716	0.093106	1.42
30	62.710	0.090872	1.99
40	61.528	0.088231	2.95
50	60.012	0.084710	4.71
60	57.988	0.079863	8.41
65	56.804	0.077022	11.8
67	56.256	0.075692	13.7
70	55.355	0.073466	17.4
75	53.650	0.069230	27.0
80	51.654	0.064246	45.0
85	49.415	0.058684	80.4
90	46.630	0.051654	160
91	46.037	0.050186	187
92	45.333	0.048385	221
93	44.796	0.047127	260
94	44.206	0.045713	308
95	43.503	0.043944	367
96	42.864	0.042414	440
97	42.166	0.040700	531
98	41.435	0.038918	648
99	40.742	0.037274	794
100	40.075	0.035730	976

* value at 0% glycerol was taken from [18].

A series of solutions of glycerol were prepared, their viscosities at 25 °C calculated using Equation (1), and their backpressure profiles measured after 10 microliter injections into the HPLC system (see Materials and Methods section for experimental details). At the first approximation, a linear relationship between logarithm of viscosity and the generated pressure was observed (Figure 3).

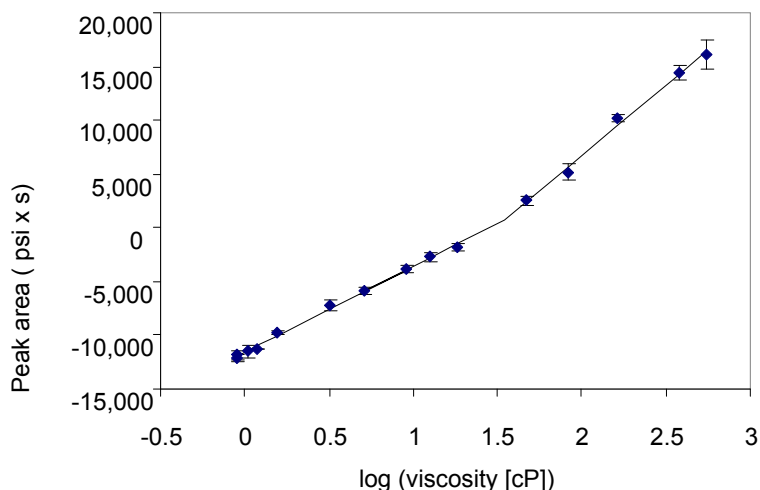
However, more detailed inspection reveals a biphasic behavior, where two linear regions of slightly different slopes are discerned. Straight lines were fitted to these regions, leading to the equations for the prediction of viscosity based on the pressure at the pump for the particular system employed. The “cross-over” abscissa (X-axis) point is given by the point of intersection of the two linear fits, calculated from the relation:

$$X = (b_2 - b_1)/(a_1 - a_2) \quad (2)$$

where b_1 , b_2 and a_1 , a_2 are the intercepts and slopes of the corresponding straight lines. The X value was 1.54, corresponding to viscosity of 35 cP. The peak area at the “cross-over” point was 702

(psi x second). Thus, for peak areas below 700, an equation $y = 7958x - 11541$ was used, and for peak area above 700, the equation was $y = 13074x - 19412$.

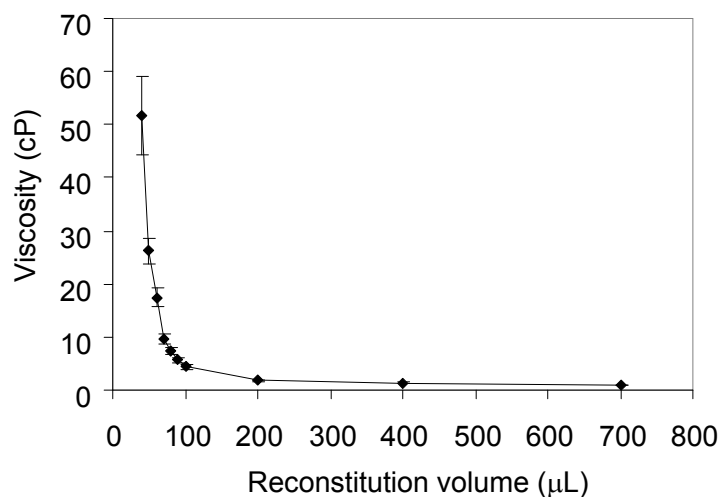
Figure 3. Calibration plot for the series of glycerol standards. Points 1–9 and 10–14 were separately fitted to a straight line by a least-squares procedure embedded in Microsoft Excel™. The error bars show the standard deviation from four measurements.



3.3. Measurement of Vaccine and Protein Samples

A series of lyophilized Varicella vaccine samples were reconstituted in decreasing volumes of USP water to estimate the highest concentration that maintained reasonable viscosity for injection. Reconstituted samples were placed in HPLC vials and the procedure was executed as described above. The resulting plot is shown in Figure 4.

Figure 4. Viscosity values of Varicella vaccine samples, reconstituted in different volumes of USP water, obtained by high-pressure liquid chromatography (HPLC) method. The error bars represent standard deviation of four measurements.



There was little increase of viscosity between reconstitution volumes of 700 μL and 100 μL . The intermediate range, where the viscosity raised sharply in decreasing reconstitution volumes, fell between 100 μL and 50 μL . At lower reconstitution volumes, the viscosity reached approximately ~ 50 cP, and the standard deviation also increased, presumably due to the presence of cell debris in the Varicella vaccine preparations, potentially leading to the interactions with surfaces in the sampling system needle and/or tubing surfaces. Furthermore, since the relationship of concentration and viscosity is non-linear, at high concentrations small differences of concentration will result in large changes of viscosity. In general, any differences of concentration between the injections that might be due to sedimentation or surface interactions will tend to increase irreproducibility.

This example illustrates the utility of this method, as a large number of measurements were made using minimal amount of sample. In fact, even smaller amounts would be difficult to handle because of evaporation effects as well as typical lesser accuracy of standard laboratory pipettes at that volume range. The experiment consisted of placing the volumes into the vials, loading the autosampler and starting the pre-programmed method within the HPLC system. After the runs were complete, the set of chromatogram files was exported into an Excel workbook, where the pre-programmed macro performed the removal of the pump pressure spikes, baseline correction, peak integration and the tabulation of the results. Thus, the entire operator's involvement was in the range of minutes rather than hours, which are often needed for traditional viscometry measurements.

Concentrated solution of bovine serum albumin (~ 100 mg/mL) was also injected into the system and the pressure was monitored as described above. No signs of increased noise, systems pressure or UV detector artifacts were observed, indicating that the partial dilution into a $\sim 70\%$ glycerol solution did not result in protein precipitation (not shown). The viscosity value, resulting from the procedure describe above, was 82 ± 5 cP. The same sample, when examined with conventional plate viscometer, yielded viscosity of 70 ± 1 cP, suggesting that some variations between the instruments should be expected.

Potential future experiments with a series of concentrated proteins at various viscosities, and examination of the corresponding UV detector profiles may help to evaluate various factors that may contribute to the method's accuracy and precision. At the present stage, however, the precision of the method allows for use as a tool in the differentiation between various proteins and formulations, in addition to obtaining approximate values of viscosity. In pharmaceutical development practice, the timing of the information and relative ranking are often of high importance, especially because often only a general qualitative range for each critical quality attribute is sought for developability assessment of therapeutic candidates.

4. Conclusions

In summary, a high-throughput, low sample volume method for the measurement of viscosity has been developed. The availability of the hardware in essentially every laboratory has the potential to make this approach widely applicable in formulation development not only of biological macromolecules, but also in any industry dealing with viscous liquids.

Acknowledgments

We would like to thank Divya Sinha for assistance with performing HPLC measurements, Jessica Sinacola for providing vaccine samples and Heidi Yoder for help with rheometry measurements.

Author Contributions

Sonia Gregory: performed the measurements, Henryk Mach: designed the study, performed measurements, analyzed the data and wrote the manuscript.

Conflicts of Interest

The authors declare no conflict of interest.

References

1. Dogan, H.; Kokini, J.L. *Handbook of Food Engineering*, 2nd ed.; CRC Press: Boca Raton, FL, USA, 2007; pp. 1–124.
2. Connelly, R.K.; Kokini, J.L. Mixing simulation of a viscous Newtonian liquid in a twin sigma blade mixer. *AIChE J.* **2006**, *52*, 3383–3393.
3. Landauer, O.; Mateescu, C.; Iulian, O.; Geana, D. Models for the viscosity of liquid mixtures—Application to the binary-system water-dioxan. *Rev. Roum. Chim.* **1987**, *32*, 1129–1139.
4. Hayduk, W.; Cheng, S.C. Review of relation between diffusivity and solvent viscosity in dilute liquid solutions. *Chem. Eng. Sci.* **1971**, *26*, 635–646.
5. Monkos, K. Determination of some hydrodynamic parameters of ovine serum albumin solutions using viscometric measurements. *J. Biol. Phys.* **2005**, *31*, 219–232.
6. Salinas, B.A.; Sathish, H.A.; Bishop, S.M.; Harn, N.; Carpenter, J.F.; Randolph, T.W. Understanding and modulating opalescence and viscosity in a monoclonal antibody formulation. *J. Pharm. Sci.* **2010**, *99*, 82–93.
7. Shire, S.J.; Shahrokh, Z.; Liu, J. Challenges in the development of high protein concentration formulations. *J. Pharm. Sci.* **2004**, *93*, 1390–1402.
8. Saluja, A.; Badkar, A.V.; Zeng, D.L.; Nema, S.; Kalonia, D.S. Application of high-frequency rheology measurements for analyzing protein–protein interactions in high protein concentration solutions using a model monoclonal antibody (IgG2). *J. Pharm. Sci.* **2006**, *95*, 1967–1983.
9. Chari, R.; Jerath, K.; Badkar, A.V.; Kalonia, D.S. Long- and short-range electrostatic interactions affect the rheology of highly concentrated antibody solutions. *Pharm. Res.* **2009**, *26*, 2607–2618.
10. Zimmer, H.; Osterr, A. Viscosity and viscosity measurements. *Chem. U. Tech. Ztg.* **1932**, *50*, 47–50.
11. Bee, J.S.; Stevenson, J.L.; Mehta, B.; Svitel, J.; Pollastrini, J.; Platz, R.; Freund, E.; Carpenter, J.F.; Randolph, T.W. Response of a concentrated monoclonal antibody formulation to high shear. *Biotechnol. Bioeng.* **2009**, *103*, 936–943.
12. Reardon, P.T.; Graham, A.L.; Feng, S.; Chawla, V.; Admuthe, R.S.; Mondy, L.A. Non-Newtonian end effects in falling ball viscometry of concentrated suspensions. *Rheol. Acta* **2007**, *46*, 413–424.

13. He, F.; Becker, G.W.; Litowski, J.R.; Narhi, L.O.; Brems, D.N.; Razinkov, V.I. High-throughput dynamic light scattering method for measuring viscosity of concentrated protein solutions. *Anal. Biochem.* **2010**, *399*, 141–143.
14. Sharma, V.K.; Kalonia, D.S. Effect of vacuum drying on protein-mannitol interactions: The physical state of mannitol and protein structure in the dried state. *AAPS Pharm. Sci. Tech.* **2004**, *5*, doi:10.1007/BF02830578.
15. Carpenter, J.F.; Randolph, T.W.; Jiskoot, W.; Crommelin, D.J.A.; Middaugh, C.R.; Winter, G.; Fan, Y.-X.; Kirshner, S.; Verthelyi, D.; Kozlowski, S.; *et al.* Overlooking subvisible particles in therapeutic protein products: Gaps that may compromise product quality. *J. Pharm. Sci.* **2009**, *98*, 1201–1205.
16. Chang, N.-S. Formula for the viscosity of a glycerol–water mixture. *Ind. Eng. Chem. Res.* **2008**, *47*, 3285–3288.
17. Dow-Chemical-Company. OPTIM Glycerine. Available online: <http://www.dow.com/glycerine/resources/table18.htm> (accessed on 12 February 2014).
18. Lide, D.R. *Viscosity in CRC Handbook of Chemistry and Physics*, 78th ed.; Lide, D.R., Ed.; CRC Press: Boca Raton, FL, USA, 1998; pp. 6–200.
19. Monkos, K.; Turczynski, B. A comparative study on viscosity of human, bovine and pig IgG immunoglobulins in aqueous solutions. *Int. J. Biol. Macromol.* **1999**, *26*, 155–159.

© 2014 by the authors; licensee MDPI, Basel, Switzerland. This article is an open access article distributed under the terms and conditions of the Creative Commons Attribution license (<http://creativecommons.org/licenses/by/3.0/>).